

Effect of Sterol Side Chain on Ion Channel Formation by Amphotericin B in Lipid Bilayers

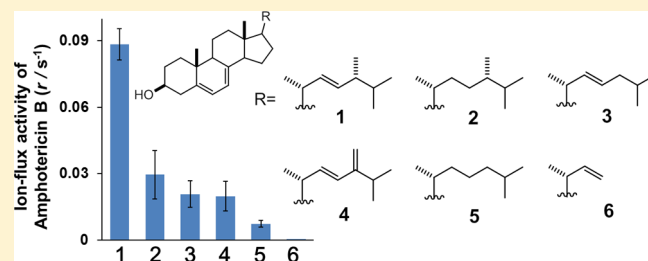
Yasuo Nakagawa, Yuichi Umegawa, Tetsuro Takano, Hiroshi Tsuchikawa, Nobuaki Matsumori,* and Michio Murata*

Department of Chemistry, Graduate School of Science, Osaka University, 1-1 Machikaneyama, Toyonaka, Osaka 560-0043, Japan

Supporting Information

ABSTRACT: Amphotericin B (AmB) is one of the most efficient antimycotic drugs used in clinical practice. AmB interacts with membrane sterols increasing permeability of fungal membranes; however, it is still unclear how AmB selectively recognizes the fungal sterol, ergosterol (Erg), over other sterols in cell membranes. In this study, we investigated the effect of an Erg side chain on AmB activity by testing a series of Erg analogues that shared the same alicyclic structure as Erg but varied in the side chain structure by using the K⁺ influx assay. The results clearly showed that the sterol side chain is essential for AmB selectivity toward Erg and for the activity of AmB-sterol ion channels.

In agreement with our previous findings showing the direct interaction between the drug and Erg, these data suggested that AmB directly recognizes the sterol side chain structure, consequently promoting the formation of ion channels by AmB. Furthermore, the C24 methyl group and Δ 22 double bond in the side chain of Erg are equally important for the interaction with AmB. Conformational analysis revealed that the C24 methyl group contributes to the interaction by increasing the van der Waals (VDW) contact area of the side chain, while the Δ 22 double bond restricts the side chain conformation to maximize the VDW contact with the rigid AmB aglycone. This study provides direct experimental evidence of the mechanism of AmB selectivity toward fungal Erg.



Amphotericin B (AmB) is the most important representative of polyene macrolide antibiotics, and it has remained the drug of choice for the treatment of life-threatening systemic fungal infections despite its serious side effects.^{1,2} It has long been established that AmB forms ion-permeable channels in fungal cell membranes in the presence of sterols,³ which disrupt membrane functions by causing cation flux across the membrane eventually leading to cell death.⁴ The selective toxicity of AmB toward fungi is thought to be underlined by its higher affinity to ergosterol (Erg)-containing fungal membranes than to cholesterol (Cho)-containing mammalian membranes.^{5,6} On the other hand, Burke's groups has recently suggested that the channel formation is a secondary mode of action and that simply binding to Erg is the critical mechanism of AmB antifungal activity, because AmB binding inhibits essential Erg functions in yeast physiology, including vacuole fusion, endocytosis, pheromone signaling, and the activity control of membrane proteins.^{7,8} Further understanding of the molecular mechanisms underlying AmB recognition of Erg should help improve the efficacy and reduce the side effects of AmB.

The molecular structure of Erg differs from that of mammalian Cho by the presence of an additional methyl group and a double bond in the side chain and another unsaturated bond in the steroid nucleus. These minor structural differences significantly increase Erg affinity to AmB compared to that of Cho—this was confirmed by experimental and

theoretical data, including UV/CD spectroscopy,^{9–12} ion-flux assays,^{10,13,14} and computational analysis.^{15–18} Although it has been assumed that π – π electronic interactions between the two extra double bonds in Erg and the heptaene moiety of AmB stabilize the drug-Erg complex,¹⁶ the details of their mutual recognition are largely unknown. In particular, the role of the side chain has not been fully investigated experimentally, although some theoretical studies have suggested that the Δ 22 double bond significantly contributes to AmB–Erg interaction by enhancing the rigidity and/or electron density of the side chain, while the methyl group at the C24 position is less important.^{15,16,19} The lack of experimental data can be attributed to the limited availability of structural derivatives of Erg from commercial sources. Since AmB–sterol interactions are known to depend heavily on membrane lipids,^{20,21} a choice of phospholipid is important for examining the membrane activity of AmB using liposomes; in the previous study, we have demonstrated that 1-palmitoyl-2-oleoyl-*sn*-glycero-3-phosphocholine (POPC) is a suitable lipid to clearly observe the sterol specificity of AmB, while 1,2-dimyristoyl-*sn*-glycero-3-phosphocholine (DMPC) membrane obscures the selectivity.²⁰ In this study, we synthesized a series of Erg analogues, which share the common alicyclic structure but differ in the side chain

Received: January 28, 2014

Revised: April 24, 2014

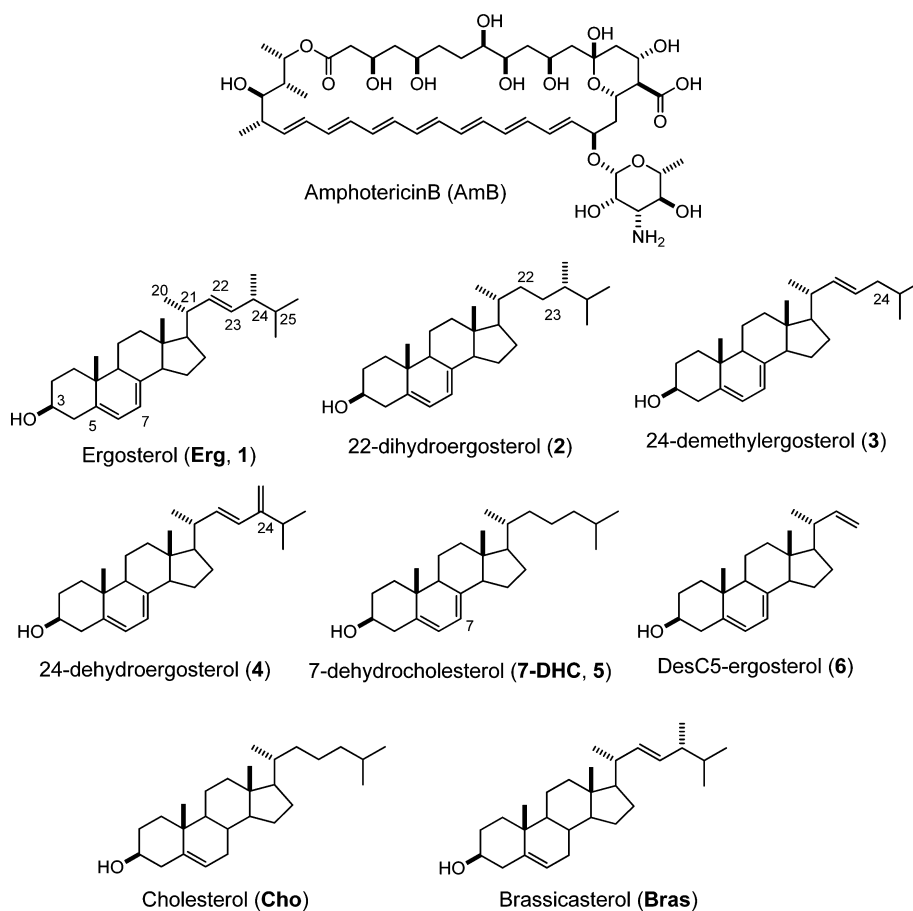


Figure 1. Chemical structures of amphotericin B and sterol analogues used in this study. Analogues 2–6 share the alicyclic structure with Erg 1, whereas Cho and brassicasterol (bottom) have a different alicyclic structure.

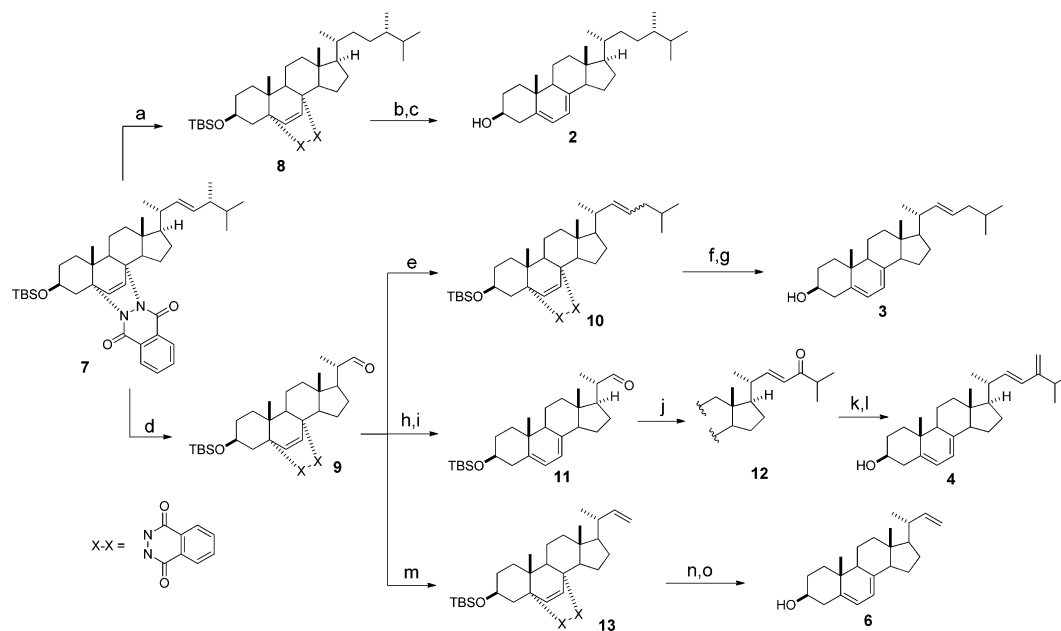
composition (Figure 1). Except for commercially available Erg and 7-dehydrocholesterol (7-DHC), the other Erg derivatives were obtained using novel synthetic schemes. Then we compared the capability of these sterols to promote AmB-induced ion flux into POPC liposomes.

MATERIALS AND METHODS

Materials. Erg analogues 22-dihydroergosterol (2), 24-demethylergosterol (3), 24-dehydroergosterol (4), and desCS-ergosterol (6) were synthesized from Erg (the detailed synthesis protocol is provided as Supporting Information). AmB, Cho, carbonyl cyanide-*p*-trifluoro-methoxy-phenyl hydrazine (FCCP), 2',7'-bis(carboxyethyl)-4(5)-carboxyfluorescein (BCECF), and valinomycin were purchased from Nacalai Tesque (Kyoto, Japan). Erg was obtained from Tokyo Kasei (Tokyo, Japan), 7-DHC was obtained from MP Biomedicals Inc. (California, USA), and POPC was obtained from NOF corp. (Tokyo, Japan). All other chemicals were obtained from standard vendors and were of analytical grade.

K⁺ Flux Assays Using BCECF. K⁺ influx induced by AmB is directly associated with H⁺-efflux from the liposomes and can be monitored as pH change inside the liposomes by fluorescence intensity of the liposome-entrapped pH sensitive dye BCECF, as described in our previous report.²² POPC and sterols, Erg 1, 22-dihydroergosterol 2, 24-demethylergosterol 3, 24-dehydroergosterol 4, 7-DHC 5, desC5-ergosterol 6, were dissolved in CHCl₃, and the solvent was evaporated to form lipid films in a round-bottom flask, which was then left under a

vacuum for over 6 h to completely remove the solvent. Lipid films thus obtained were hydrated with phosphate buffer (0.15 M potassium phosphate and 0.76 μM BCECF, pH 5.8) by sonication and vortexing. The resultant suspension was frozen at –20 °C and thawed at 60 °C five times to form large vesicles. After the sizing of the liposomes by stepwise extrusion (19 times) through a polycarbonate filter (200 nm pore size) using a syringe extruder Liposfast (AVESTIN Inc., Ottawa, Canada), the resultant BCECF-entrapping liposomes yielding mostly large unilamellar vesicles (LUVs) were separated from the remaining BCECF by gel filtration using Sepharose 4B (Sigma-Aldrich, St. Louis, MO) and 0.15 M potassium phosphate buffer (pH 5.8). Lipid concentration in the liposomes was determined by phospholipids C (Wako Pure Chemical Industries, Ltd., Japan), and the liposome suspension was diluted with the same buffer to 0.5 mM lipid concentration. To monitor the potassium–proton exchange, a 50 μL aliquot of 1 mM FCCP was added to 5 mL of liposome suspension stored at 6 °C. The suspension (200 μL) was added to a cuvette containing 1.8 mL of K₂HPO₄ (0.15 M), which was positioned in a fluorescence spectrometer (FP-6600, JASCO, Tokyo, Japan). After addition of 10 μL of 32 μM AmB in DMSO (a final concentration of AmB was 0.16 μM), the time-dependent change in the liposomal pH was monitored by the increase in the fluorescence intensity (excitation, 500 nm and emission, 535 nm) at 6 °C. The initial pH values of the liposome suspension and liposome lumen were 7.8 and 5.8, respectively. Valinomycin in aqueous solution (5 mM, 10 μL) was added to

Scheme 1. Reagents and Conditions^a

^a(a) Pd-C, AcOEt, room temperature (rt), 5 h; (b) LiAlH₄, THF, reflux, 2 h; (c) TBAF, rt, overnight, then HPLC purification, 10% from 7; (d) O₃, pyridine, CH₂Cl₂, -78 °C, then Me₂S, 86%; (e) 5-(isopentylsulfonyl)-1-phenyl-1H-tetrazole, KHMDS, THF, -78 °C → rt, overnight, 44% (*E/Z* = 6/1); (f) LiAlH₄, THF, reflux, 2 h; (g) TBAF, THF, rt, overnight, then HPLC purification, 69% from 10; (h) LiAlH₄, THF, reflux, 2 h, 56%; (i) SO₃-Py, Et₃N, DMSO, CH₂Cl₂, rt, 2 h, 93%; (j) 3-methyl-2-oxo-butylphosphonate, *t*-BuOK, THF, 0 °C → reflux, 96%; (k) CH₃PPh₃Br, *t*-BuOK, THF, 0 °C → reflux, 91%; (l) TBAF, THF, rt, overnight, 85%; (m) CH₃PPh₃Br, *t*-BuOK, THF, 0 °C → rt, overnight, 96%; (n) LiAlH₄, THF, reflux, 1.5 h; (o) TBAF, THF, rt, overnight, 71% for 2 steps.

obtain the fluorescence intensity corresponding to 100% exchange (F_{\max}); the following changes in fluorescence intensity were normalized to F_{\max} .

For the preincubation experiment, 200 μ L of liposome suspension was mixed with 10 μ L of 32 μ M AmB in DMSO and 2.0 μ L of 1 mM FCCP in EtOH and incubated for 3 h at 6 °C. The suspension was added to the cuvette containing 1.8 mL of K₂HPO₄ (0.15 M) positioned in the fluorescent spectrometer. After the addition of liposome suspension, the time course of pH change in the liposomes was monitored and expressed as the percentage to that of F_{\max} as described above.

Surface Plasmon Resonance (SPR). The experiments were performed as described in our previous report.²³ Briefly, the liposome solution was prepared with POPC (4 μ mol) and sterols (1 μ mol) mixed in CHCl₃. After removal of the solvent, the film was hydrated with PBS buffer, vortexed, and sonicated, yielding multilamellar vesicles. The suspension was subjected to several cycles of freezing, thawing, and vortexing to obtain LUVs, which were passed through a 100 nm polycarbonate filter and diluted to the final lipid concentration of 0.25 mM. SPR measurements were carried out at 25 °C using the CMS sensor chip mounted in a BIAcore T200 analytical system (BIAcore AB, Uppsala, Sweden). The experimental details are provided as Supporting Information.

Molecular Modeling of the Sterol Side Chain. The conformational search and multiple minimizations were carried out using the MacroModel software version 9.3.5 installed in the Windows 7 operating system. Sampling of the conformational space was performed with a mixed torsional/low-mode sampling (MCM/LMCS).²⁴ The OPLS 2005 force field²⁵ implemented in the MacroModel program was used for the conformational searches in 5000 steps. Energy minimization was carried out by using the Polak-Ribiere conjugate gradient

(PRCG) method with 7000 maximum iterations. The resultant structures were then minimized, and redundant conformers were eliminated. Energy minimization was carried out by using the truncated newton conjugate gradient (TNCG) method with 7000 maximum iterations.

RESULTS

Synthesis of Sterol Analogues. Erg analogues 2, 3, 4, and 6 were synthesized via common intermediate 7²⁶ (Scheme 1). The synthesis of 22-dihydroergosterol 2 commenced with the direct hydrogenation of 7 to provide an inseparable mixture of the products carrying the unsaturated (8) and saturated 6,7-bond. Deprotection of the diene group and removal of *tert*-butyldimethylsilyl (TBS) group gave a mixture of 22-dihydroergosterol 2 and the saturated azo-adduct without TBS, which could be readily separated by silica gel column chromatography. The other analogues were successfully synthesized from aldehyde 9 by the introduction of the corresponding side chains. Julia-Kocienski coupling between aldehyde 9 and 5-(isopentylsulfonyl)-1-phenyl-1H-tetrazole²⁷ afforded 10 as an inseparable mixture of *E/Z* = 6/1. After deprotection, HPLC purification yielded 24-demethylergosterol 3 as a single isomer. For the synthesis of 24-dehydroergosterol 4, although the Horner–Wadsworth–Emmons reaction between aldehyde 9 and 3-methyl-2-oxo-butylphosphonate²⁸ was unsuccessful, it occurred smoothly between phosphonate and deprotected aldehyde 11 to produce the desired ketone 12 with good yield. Subsequent Wittig methylenation of ketone 12, followed by removal of the TBS group, yielded 24-dehydroergosterol 4. DesC₅-ergosterol 6 was synthesized by the direct methylenation of aldehyde 9 and subsequent deprotection of the diene and hydroxy groups.

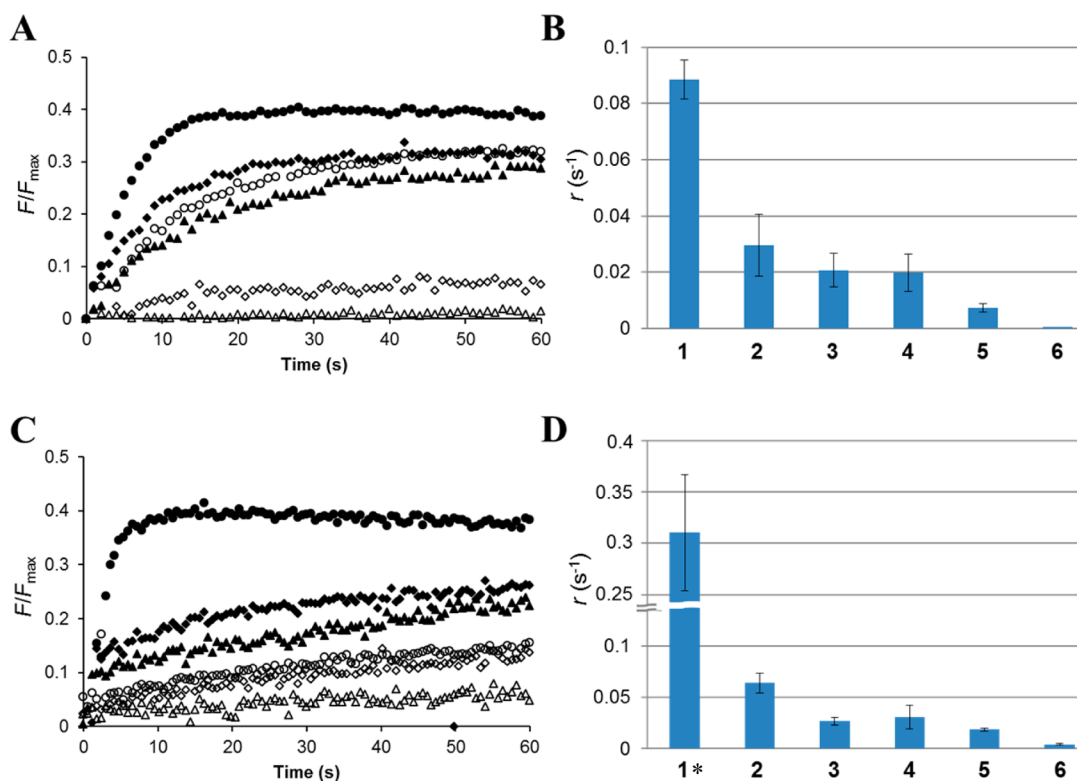


Figure 2. Effect of Erg analogues on AmB-induced K⁺ influx. Fluorescence intensity (F/F_{\max}) was monitored with the pH-sensitive dye BCECF. The liposomes were prepared from POPC mixed with 5 mol % Erg (1) ●, 22-dihydroergosterol (2) ◆, 24-demethylergosterol (3) ○, 24-dehydroergosterol (4) ▲, 7-DHC (5) ◇, and desC₅-ergosterol (6) △. The results are presented at $R_{(\text{AmB}/\text{lipid})} = 3.16 \times 10^{-3}$. A: at 0 s, AmB in DMSO (final DMSO concentration below 1%) was added to the liposomes. C: AmB was preincubated with the liposomes for 3 h before the fluorescence recording, and then the pH gradient was formed by raising the pH of the liposome suspension. B and D: K⁺/H⁺ exchange rate (r) obtained from the experiments A and C, respectively, and calculated by fitting to the exponential curve ($F = A(1 - \exp(-t/T))$); r immediately after adding AmB was presented as $\Delta F = A/T$ ($t = 0$). The initial fluorescence values for 60 and 20 s were used for the fitting analysis of A and C data, respectively. *The initial rate of the fluorescence change for Erg in panel D was too fast to obtain accurate values.

K⁺ Influx Assays. For evaluating the membrane-permeabilizing activity of AmB, usual fluorescence assays such as dye-leakage from liposomes cannot be used because the pore formed by membrane-bound AmB and sterol is too small to pass a dye molecule. We have devised a new fluorescence method to measure K⁺ flux into liposomes by monitoring pH change with a pH-dependent fluorescent dye, BCECF.²² In the present study, we carried out this K⁺ influx measurement in two different ways to investigate the effect of the sterol side chain on the activity—one focused on the early stage of AmB–sterol complex formation (Figure 2A,B) and the other on the steady state after 3 h incubation (Figure 2C,D). As shown in Figure 2A,C, any changes in the side chain structure significantly reduced the K⁺ influx activity of AmB, clearly indicating that the side chain in Erg (1) afforded the highest level of AmB-induced membrane permeabilization among the tested sterols (Figure 2A,C). As seen in the results of the same flux assays with the sterol content of 10 mol % in Supporting Information, the relative potency of the sterol analogues in stimulating AmB-induced K⁺ flux was not significantly changed at higher sterol content in liposomes.

In the early stage experiments, K⁺/H⁺ exchange rates were calculated from the changes in fluorescence intensity immediately after AmB addition by curve fitting (Figure 2B). It was found that 3 and 4, which lacked the 24-methyl group and Δ22-double bond, respectively, showed significantly reduced K⁺/H⁺ exchange compared to Erg (1). Consistently,

further reduction of K⁺ influx was observed for the liposomes containing 5, which lacked both the 24-methyl group and the Δ22-double bond. Interestingly, the replacement of the 24-methyl group with exomethylene (4), which was expected to enhance π–π electronic interaction with AmB, rather reduced the activity to the level comparable to that of the 24-demethyl derivative. In both experiments presented in Figure 2, almost no K⁺/H⁺ exchange was observed for the membrane containing desC₅-ergosterol 6 that lacked a large part of the side chain structure 1.

Figure 2D shows the K⁺-flux activity in the liposomes after 3 h incubation with AmB, which was similar to the results in Figure 2B for all the derivatives (2–6), implying that the side chain played roles both in the binding to AmB-containing membrane and in the stabilization of the AmB–sterol complex in the membrane; the former is clearly illustrated by the exchange rates presented in Figure 2A,B, while the latter can be better evaluated after longer incubation times, as shown in Figure 2C,D. The detailed comparison, however, revealed certain dissimilarity between A/B and C/D. The differences between the flux-promoting activity of Erg and other sterols were more pronounced after 3 h incubation compared to that without incubation, suggesting that the side chain structure contributed to the stabilization of the AmB–sterol complex rather than to the binding of AmB to the membrane.

SPR-Based Affinity Assays. To further evaluate the impact of the side chain on AmB–sterol interaction in comparison, we

carried out SPR experiments for Erg (1), its analogues 2, 3, 5, and brassicasterol and Cho (Figure 1) using a sensor chip coated with the sterol-containing POPC membranes. Since the kinetic parameters in the association step of AmB such as the association rate constant k_{a1} are known to be significantly influenced by the experimental conditions, particularly the concentration of AmB and the amount of membrane lipids immobilized on the sensor chip,^{23,29} we examined the lifetime of the AmB-sterol complex using the dissociation time constant T_{d2} (Figure 3). The results appeared to be similar to those

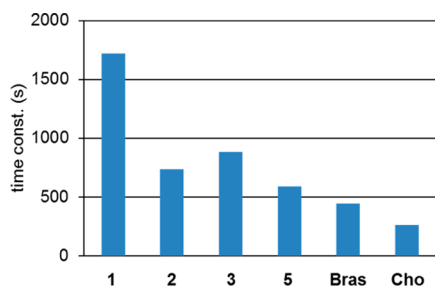


Figure 3. Lifetime of the AmB–sterol complexes evaluated by the time constant of dissociation T_{d2} (experimental details and sensorgrams are provided as Supporting Information). Bras (brassicasterol) and Cho have a difference structure in their alicyclic portion from that of Erg.

obtained in the K^+ influx assays (Figure 2B,D). Interestingly, brassicasterol, which has the same side chain as Erg and the same alicyclic structure as Cho showed weak affinity to AmB, similar to that of 7-DHC (5), which has the opposite structural relationships. Thus, their comparable lifetimes may indicate that the higher affinity to AmB of Erg compared to Cho is underlined by the additional unsaturated bond in the ring B as well as by the difference in the side-chain structure. The data on the K^+ flux activity of brassicasterol and other sterol analogues with different cyclic structures will be published elsewhere.

DISCUSSION

In order to investigate the effect of the sterol side chain on the membrane-permeabilizing activity of AmB, we synthesized a series of Erg derivatives with different side chain structures, incorporated them in the liposomes, and analyzed them in the K^+ influx assay. The results clearly demonstrated that AmB-induced ion-channel formation depended on the structure of the sterol side chain. Given our previous data obtained by solid state NMR showing that Erg directly bound to AmB in hydrated lipid bilayers,^{20,26} it is reasonable to deduce that the sterol side chain is directly involved in the interaction between sterols and AmB, which consequently influences membrane permeabilization by AmB.

The dependency of AmB binding affinity on the structure of the sterol side chain indicates that upon the binding to the membrane, AmB recognizes the sterol side chain residing deep in the hydrophobic interior of the membrane bilayer. This is in sharp contrast to the mode of action of other sterol-binding natural products such as theonellamides and amphidinol 3, which largely interact with the shallowly embedded 3-OH group of the sterol A-ring and therefore show less dependency on the side chain structure.^{30,31} A possible explanation for AmB recognition of the side chain during the membrane binding is that the drug enters into the membrane interior to interact with the sterol side chain rather than shallowly embedded on the membrane surface as revealed by our solid-state NMR

experiments;²⁶ this stable interaction between the sterol side chain and the hydrophobic portion of AmB is plausibly caused by their contact with larger areas of the molecular surface as discussed below.

The ordering effect induced by sterols is another important factor to influence the binding affinity of AmB to lipid bilayers. Hsueh et al. measured the first moment of quadrupolar splitting of POPC- d_{31} to evaluate the ordering of an acyl chain in membrane containing 10% Cho, 7-DHC or Erg³² and reported that these three sterols gave rise to a similar effect while Cho is slightly higher than 7-DHC (5) or Erg, which was opposite to that of AmB-affinity shown in Figure 3. AmB is known to have higher affinity to ordered membrane,^{33,34} thus implying that the affinity of AmB to sterol-containing membranes is due not to membrane ordering but largely to AmB–sterol interaction.

The present results also clearly demonstrate that both methyl groups at C24 and the double bond between C22 and C23 in Erg are important for the affinity to AmB. Previous studies, including the recent one by Neumann et al.,³⁵ have suggested that van der Waals (VDW) forces are essential for the interaction of AmB with membrane sterols;^{14–18,36,37} therefore the weak channel activity and low AmB affinity of demethyl analogue 3 can be explained by a loss of the VDW contact area in the side chain. However, the difference in the VDW force alone seems insufficient to explain the lower activity of 2 and 4, which have the same bulky side chains as Erg. Baginski's group has reported that Cho has higher conformational flexibility of the side chain compared to Erg;³⁸ therefore, it is not far-fetched to assume that the conformation of the side chain is partially responsible for the lower Cho affinity to AmB and less favored VDW interaction with the rigid AmB aglycone. We compared the conformational preferences of each sterol analogue. Figure 4 shows the superposition of sterol derivatives in a window of 5 kJ mol^{-1} calculated by a conformational search algorithm (see Methods). The major difference resides in the C17–C20–

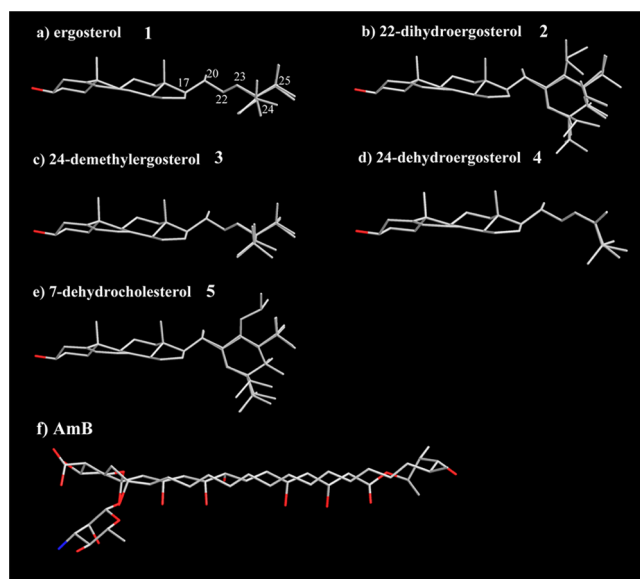


Figure 4. Structure superposition of sterol derivatives within a window of 5 kJ mol^{-1} from the ground minimum (generated by conformational search followed by multiple minimization) (a–e). A total of 15, 27, 18, 7, and 30 conformers for 1, 2, 3, 4, and 5 were generated, and each model was superposed for the minimum RMSD at the steroid ring. (f) X-ray crystal structure of AmB.³⁹

C22–C23 dihedral angle of the sterols bearing the C22–C23 unsaturated bond (Figure 4, 1, 3, and 4), which is around -120° , while that of the saturated sterols (2 and 5) is around 60° . Due to this conformational difference, the saturated side chains of 2 and 5 tend to have perpendicular orientation to the plane of the steroid rings, which would decrease their affinity for the rigid AmB aglycone (Figure 3).

Meanwhile, the lower activity of 4 may contradict the previous data on the significance of π – π electronic interaction between the AmB polyene chromophore and the sterol side chain.¹⁶ The conformation in Figure 4 may provide an explanation to its low activity; the conjugated diene moiety forces *s-trans* conformation of the C23–C24 bond, and the resultant orientation of the terminal portion, which is different from that of 1, would hinder the VDW contact with AmB. These results confirm that the VDW interaction between the rigid AmB aglycone and the sterol side chain is critical for the formation of functional AmB–sterol ion channels. The C24 methyl group contributes to the VDW contact of the side chain with AmB, whereas the Δ 22 double bond restricts the side chain in the conformation suitable for interaction with AmB.

CONCLUSIONS

In this study, we performed ion-flux assays and SPR measurements using Erg derivatives with various structures of the side chain and showed that the 24-methyl group and the Δ 22 double bond in the side chain are required for the affinity to AmB and the formation and functional activity of the sterol–AmB ion channels. The present data imply that AmB directly recognizes the sterol side chain, consequently promoting the formation of ion channels with AmB. We also show that both the C24 methyl group and the Δ 22 double bond independently influence AmB–sterol interaction. Conformational analysis of different side chain structures suggests that the C24 methyl group functions to increase the VDW contact area of the side chain, and the Δ 22 double bond restricts the side chain to the conformation suitable for the VDW contact with AmB. The findings of this study provide important insight for a better understanding of bimolecular interaction between AmB and sterols.

ASSOCIATED CONTENT

Supporting Information

Experimental details of synthesis of Erg analogues and SPR experiments. This material is available free of charge via the Internet at <http://pubs.acs.org>.

AUTHOR INFORMATION

Corresponding Authors

*(M.M.) Phone (+81)-6-6850-5774. Fax (+81)-6-6850-5774. E-mail murata@chem.sci.osaka-u.ac.jp.

*(N.M.) Phone (+81)-6-6850-5790. Fax (+81)-6-6850-5789. E-mail matsmori@chem.sci.osaka-u.ac.jp.

Funding

This study was partly supported by Grant-In-Aids for Scientific Research (A) (No. 25242073) and for Young Scientists (B) (No. 25750383) from MEXT, Japan, and also in part as “Lipid-acting Structure Project (ERATO)” from Japan Science and Technology Agency.

Notes

The authors declare no competing financial interest.

ACKNOWLEDGMENTS

Y.N. as a JSPS fellow is grateful to Japan Society for the Promotion of Science. A research fellowship to T.T. from the GCOE program, “Global Education and Research Center for Bio-Environmental Chemistry,” is also acknowledged.

ABBREVIATIONS

AmB, amphotericin B; BCECF, 2',7'-bis(carboxyethyl)-4(5)-carboxyfluorescein; Bras, brassicasterol; Cho, cholesterol; 7-DHC, 7-dehydrocholesterol; DMPC, 1,2-dimyristoyl-*sn*-glycero-3-phosphocholine; Erg, ergosterol; FCCP, carbonyl cyanide-*p*-trifluoro-methoxy-phenyl hydrazine; POPC, 1-palmitoyl-2-oleoyl-*sn*-glycero-3-phosphocholine; SPR, surface plasmon resonance; TBS, *tert*-butyldimethylsilyl

REFERENCES

- (1) Gallis, H. A., Drew, R. H., and Pickard, W. W. (1990) Amphotericin B: 30 years of clinical experience. *Rev. Infect. Dis.* 12, 308–329.
- (2) Lemke, A., Kiderlen, A. F., and Kayser, O. (2005) Amphotericin B. *Appl. Microbiol. Biotechnol.* 68, 151–162.
- (3) Kruijff, B. D., and Demell, R. A. (1974) Polyene antibiotic-sterol interactions in membranes of *Acholeplasma laidlawii* cells and lecithin liposomes. III. Molecular structure of the polyene antibiotic-cholesterol complexes. *Biochim. Biophys. Acta* 339, 57–70.
- (4) Bolard, B. (1986) How do the polyene macrolide antibiotics affect the cellular membrane properties? *Biochim. Biophys. Acta* 864, 257–304.
- (5) Zotchev, S. B. (2003) Polyene Macrolide Antibiotics and their Applications in Human Therapy. *Curr. Med. Chem.* 10, 211–223.
- (6) Baginski, M., Czub, J., and Sternal, K. (2006) Interaction of amphotericin B and its selected derivatives with membranes: molecular modeling studies. *Chem. Rec.* 6, 320–332.
- (7) Palacios, D. S., Dailey, I., Siebert, D. M., Wilcock, B. C., and Burke, M. D. (2011) Synthesis-enabled functional group deletions reveal key underpinnings of amphotericin B ion channel and antifungal activities. *Proc. Natl. Acad. Sci. U.S.A.* 108, 6733–6738.
- (8) Gray, K. C., Palacios, D. S., Dailey, I., Endo, M. M., Uno, B. E., Wilcock, B. C., and Burke, M. D. (2012) Amphotericin primarily kills yeast by simply binding ergosterol. *Proc. Natl. Acad. Sci. U.S.A.* 109, 2234–2239.
- (9) Charbonneau, C., Fournier, I., Dufresne, S., Barwicz, J., and Tancrède, P. (2001) The interactions of amphotericin B with various sterols in relation to its possible use in anticancer therapy. *Biophys. Chem.* 91, 125–133.
- (10) Vertut-Croquin, A., Bolard, J., Chabbert, M., and Gary-Bobo, C. (1983) Differences in the interaction of the polyene antibiotic amphotericin B with cholesterol- or ergosterol-containing phospholipid vesicles. A circular dichroism and permeability study. *Biochemistry* 22, 2939–2944.
- (11) Clejan, S., and Bittman, R. (1985) Rates of amphotericin B and filipin association with sterol. *J. Biol. Chem.* 260, 2884–2889.
- (12) Chen, W. C., and Bittman, R. (1977) Kinetics of association of amphotericin B with vesicles. *Biochemistry* 16, 4145–4149.
- (13) Gary-Bobo, C. M. (1989) Polyene-sterol interaction and selective toxicity. *Biochimie* 71, 37–47.
- (14) Hsueh, C., and Feingold, D. (1973) Selective membrane toxicity of polyene antibiotics: study on lecithin membrane models (liposomes). *Antimicrob. Agents Chemother.* 4, 309–315.
- (15) Baginski, M., Resat, H., and Borowski, E. (2002) Comparative molecular dynamics simulations of amphotericin B-cholesterol/ergosterol membrane channels. *Biochim. Biophys. Acta* 1567, 63–78.
- (16) Baran, M., Borowski, E., and Mazerski, J. (2009) Molecular modeling of amphotericin B-ergosterol primary complex in water II. *Biophys. Chem.* 141, 162–168.
- (17) Neumann, A., Baginski, M., and Czub, J. (2010) How do sterols determine the antifungal activity of amphotericin B? Free energy of

binding between the drug and its membrane targets. *J. Am. Chem. Soc.* 132, 18266–18272.

(18) Neumann, A., Czub, J., and Baginski, M. (2009) On the possibility of the amphotericin B-sterol complex formation in cholesterol- and ergosterol containing lipid bilayers: A molecular dynamics study. *J. Phys. Chem. B* 113, 15875–15885.

(19) Baginski, M., Bruni, P., and Borowski, E. (1994) Comparative analysis of the distribution of the molecular electrostatic potential for cholesterol and ergosterol. *J. Mol. Struct. Theochem.* 311, 285–296.

(20) Matsumori, N., Tahara, K., Yamamoto, H., Morooka, A., Doi, M., Ohishi, T., and Murata, M. (2009) Direct interaction between amphotericin B and ergosterol in lipid bilayers as revealed by ^2H NMR spectroscopy. *J. Am. Chem. Soc.* 131, 11855–11860.

(21) Dufourc, E. J., Smith, I. C. P., and Jarrell, H. C. (1984) Amphotericin and model membranes; the effect of amphotericin B on cholesterol-containing systems as viewed by ^2H -NMR. *Biochim. Biophys. Acta* 776, 317–329.

(22) Takano, T., Konoki, K., Matsumori, N., and Murata, M. (2009) Amphotericin B-induced ion flux is markedly attenuated in phosphatidylglycerol membrane as evidenced by a newly devised fluorometric method. *Bioorg. Med. Chem.* 17, 6301–6304.

(23) Mouri, R., Konoki, K., Matsumori, N., Ohishi, T., and Murata, M. (2008) Complex formation of amphotericin B in sterol-containing membranes as evidenced by surface plasmon resonance. *Biochemistry* 47, 7807–7815.

(24) Kolossvary, I., and Guida, W. C. J. (1999) Low-mode conformational search elucidated: Application to C39H80 and flexible docking of 9-deazaguanine inhibitors into PNP. *Comp. Chem.* 20, 1671–1684.

(25) Kaminski, G. A., Friesner, R. A., Tirado-Rives, J., and Jorgensen, W. J. (2001) Evaluation and reparametrization of the OPLS-AA force field for proteins via comparison with accurate quantum chemical calculations on peptides. *J. Phys. Chem. B* 105, 6474–6487.

(26) Umegawa, Y., Nakagawa, Y., Tahara, K., Matsumori, N., Ohishi, T., and Murata, M. (2012) Head-to-tail interaction between amphotericin B and ergosterol occurs in hydrated phospholipid membrane. *Biochemistry* 51, 83–89.

(27) Fettes, A., and Carreira, E. M. (2003) Leucascandrolide A: Synthesis and related studies. *J. Org. Chem.* 68, 9274–9283.

(28) Lundy, B. J., Popova, S. J., and May, J. A. (2011) Enantioselective conjugate addition of alkenylboronic acids to indole-appended enones. *Org. Lett.* 13, 4958–4961.

(29) Onishi, M., and Kaminori, H. (2013) High-Throughput and sensitive assay for amphotericin B interaction with lipid membrane on the model membrane systems by surface plasmon resonance. *Biol. Pharm. Bull.* 36, 658–663.

(30) Espiritu, R. A., Matsumori, N., Murata, M., Nishimura, S., Kakeya, H., Matsunaga, S., and Yoshida, M. (2013) Interaction between the marine sponge cyclic peptide theonellamide A and sterols in lipid bilayers As viewed by surface plasmon resonance and solid-state ^2H nuclear magnetic resonance. *Biochemistry* 52, 2410–2418.

(31) Kasai, Y., Matsumori, N., Ueno, H., Nonomura, K., Yano, S., Murata, M., and Oishi, T. (2011) Synthesis of 6-F-ergosterol and its influence on membrane-permeabilization of amphotericin B and amphidinol 3. *Org. Biomol. Chem.* 9, 1437–1442.

(32) Hsueh, Y. W., Chen, M. T., Patty, P. J., Code, C., Cheng, J., Frisken, B. J., Zuckermann, M., and Thewalt, J. (2007) Ergosterol in POPC membranes: Physical properties and comparison with structurally similar sterols. *Biophys. J.* 92, 1606–1615.

(33) Bolard, J., Vertut-Croquin, A., Cnbulska, B. E., and Gary-Bobo, C. M. (1981) Transfer of the polyene antibiotic amphotericin B between single-walled vesicles of dipalmitoyl-phosphatidylcholine and egg-yolk phosphatidylcholine. *Biochim. Biophys. Acta* 647, 241–248.

(34) Matsuoka, S., and Murata, M. (2002) Cholesterol markedly reduces ion permeability induced by membrane-bound amphotericin B. *Biochim. Biophys. Acta* 1564, 429–434.

(35) Neumann, A., Baginski, M., and Czub, J. (2010) How do Sterols determine the antifungal activity of amphotericin B? Free energy of

binding between the drug and its membrane targets. *J. Am. Chem. Soc.* 132, 18266–18272.

(36) Kasai, Y., Matsumori, N., Umegawa, Y., Matsuoka, S., Ueno, H., Ikeuchi, H., Ohishi, T., and Murata, M. (2008) Self-assembled amphotericin B is probably surrounded by ergosterol: bimolecular interactions as evidenced by solid-state NMR and CD spectra. *Chem.—Eur. J.* 14, 1178–1185.

(37) Langlet, J., Berges, J., Caillet, J., and Demaret, J. P. (1994) Theoretical study of the complexation of amphotericin B with sterols. *Biochim. Biophys. Acta* 1191, 79–93.

(38) Czub, J., and Baginski, M. (2006) Comparative molecular dynamics study of lipid membranes containing cholesterol and ergosterol. *Biophys. J.* 90, 2368–2382.

(39) Jarzemska, K. N., Kaminski, D., Hoster, A. A., Malinska, M., Senczyna, B., Wozniak, K., and Gagos, M. (2012) Controlled crystallization, structure, and molecular properties of iodoacetyl-amphotericin B. *Cryst. Growth Des.* 12, 2336–2345.